Biosensors and Bioelectronics 36 (2012) 62–68

Contents lists available at SciVerse ScienceDirect

Biosensors and Bioelectronics

journal homepage: www.elsevier.com/locate/bios

Highly-sensitive and label-free indium phosphide biosensor for early phytopathogen diagnosis

Alberto L.D. Moreau [a,*,1], Richard Janissen [a,1], Clelton A. Santos [b], Luis A. Peroni [c], Dagmar R. Stach-Machado [c], Alessandra A. de Souza [d], Anete P. de Souza [b], Mônica A. Cotta [a]

[a] Instituto de Fisica Gleb Wataghin, Universidade Estadual de Campinas, 13083-859, Campinas, SP, Brazil
[b] Centro de Biologia Molecular e Engenharia Genética, Universidade Estadual de Campinas, 13083-875 Campinas, SP, Brazil
[c] Instituto de Biologia, Universidade Estadual de Campinas, 13083-862 Campinas, SP, Brazil
[d] Centro APTA Citros Sylvio Moreira, Instituto Agronômico, 13469-970 Cordeirópolis, SP, Brazil

ARTICLE INFO

Article history:
Received 28 November 2011
Received in revised form
23 March 2012
Accepted 26 March 2012
Available online 6 April 2012

Keywords:
Immunosensor
Field-effect transistor
Chemical functionalization
Citrus Tristeza Virus
Xylella fastidiosa
Phytopathogen

ABSTRACT

The development of highly-sensitive and label-free operating semiconductor-based, biomaterial detecting sensors has important applications in areas such as environmental science, biomedical research and medical diagnostics. In the present study, we developed an Indium Phosphide (InP) semiconductor-based resistive biosensor using the change of its electronic properties upon biomaterial adsorption as sensing element. To detect biomaterial at low concentrations, the procedure of functionalization and covalent biomolecule immobilization was also optimized to guarantee high molecule density and high reproducibility which are prerequisite for reliable results. The characterization, such as biomolecular conjugation efficiency, detection concentration limits, receptor:ligand specificity and concentration detection range was analyzed by using three different biological systems: i) synthetic dsDNA and two phytopathogenic diseases, ii) the severe CB-form of *Citrus Tristeza Virus* (CTV) and iii) *Xylella fastidiosa*, both causing great economic loss worldwide. The experimental results show a sensitivity of 1 pM for specific ssDNA detection and about 2 nM for the specific detection of surface proteins of CTV and *X. fastidiosa* phytopathogens. A brief comparison with other semiconductor based biosensors and other methodological approaches is discussed and confirms the high sensitivity and reproducibility of our InP based biosensor which could be suitable for reliable early infection diagnosis in environmental and life sciences.

1. Introduction

The development of highly-sensitive and label-free operating biosensors with conjugated biomolecules has important applications in areas such as environmental science, biomedical research and medical diagnostics (Lazcka et al., 2007; Su et al., 2011; Xue et al., 2011). Due to difficulties associated with the sensitivity, reproducibility, chemical stability, and non-specific physisorption of biomolecules to surfaces such biosensors are not available from commercial sources. In order to circumvent these problems new approaches have to be developed to create new biosensor platforms. Most biosensing devices rely on metal-oxide-semiconductor structures based on silicon (Gonçalves et al., 2008; Jane et al., 2009; Lazcka et al., 2007; Nicu and Leïchlé, 2008); few studies have used III–V semiconductors for biomolecular detection. In fact, several studies indicate that these materials show a high sensitivity to detect gases (Chattopadhyay et al., 2009; Kimura et al., 2006; Wierzbowska et al., 2008), due to the ample conductance change upon gas adsorption. In particular, for gas detection, Indium Phosphide (InP) is more convenient as potentiometric and amperometric sensor than silicon (Sato et al., 2010; Talazac, 2001). So far, for biomolecular detection applications in liquid environment, n-type InP porous nanostructures were successfully used to detect a glucose oxidase enzyme (Sato et al., 2010). In this study we show the development of a new type of resistive biosensor using InP as biosensing platform for liquid environment.

In the general context of semiconductor biosensors, the surface properties and, consequently, the functionalization quality play an increasingly important role for the overall device sensing behavior (Sturzenegger et al., 1999). A standard method of semiconductor surface functionalization specify the use of alkoxysilanes by esterification of surface silanole groups to create amino grafting sites for further biomaterial immobilization (Lenci et al., 2010; Logatcheva and Horton, 2008). However, non-homogeneous and micro-structured poly(siloxane) surface coatings are frequently obtained (Vandenberg et al., 1991; Wang et al., 1992; Wang and Jones, 1993). Surface

* Corresponding author. Tel.: +55 19 35215360; fax: +55 19 35215343.
E-mail address: amoreau@ifi.unicamp.br (A.L.D. Moreau).
[1] Author contributions: These authors contributed equally to this work.

0956-5663/$ - see front matter © 2012 Elsevier B.V. All rights reserved.
http://dx.doi.org/10.1016/j.bios.2012.03.038

functionalization using ethanolamine hydrochloride is described in the literature (Ebner et al., 2007) as an alternative method to create an acceptable number of amino grafting sites. In contrast to published work (Sturzenegger et al., 1999; Park and Ivanisevic, 2007; Zerulla and Chassé, 2009) regarding InP functionalization, in this study ethanolamine and poly(ethylene glycol) (PEG) were used to ensure a homogeneous, dense and reproducible immobilization of DNA, peptides and proteins (Janissen et al., 2009).

Physically and chemically inert linear PEG chains have been commonly used as flexible linkers to attach single biomolecules to different surfaces (Albrecht et al., 2003; Hinterdorfer et al., 2002; Kamruzzahan et al., 2006; Walsh et al., 2001). These linkers allow a rapid and free re-orientation of the attached receptor biomolecule and also shield the surface from non-specific physisorption (Blank et al., 2003; Yong-Mei et al., 2007). The carboxylic group of the custom-synthesized heterobifunctional NHS-PEG-COOH (N-hydroxysuccinimide-PEG-carboxylic acid) applied here can be used to immobilize different types of biomolecules and reacts non-specifically less often compared to the more commonly used amino and aldehyde end groups (Janissen et al., 2009; Krautbauer et al., 2003; Lindroos et al., 2001).

The sensing element of this biosensing device is the change of the electronic properties of the crystalline semiconductor (Seker et al., 2000) due to the immobilized biomaterial on the surface and can be compared with the operation of a field-effect transistor (FET) in which the channel of charge carriers is controlled capacitively by an electric field (Fig. 1).

In an n-type device as used in this study, a negative voltage of the gate causes an expansion of the depletion region width and pinches off the conduction channel, reducing the flow of charge carriers. Consequently, the change in gate voltage also changes the resistance of the conduction channel while the source-drain current is proportional to the applied voltage within a voltage range, in which case the device is operating under linear ohmic regime (Galup-Montoro and Schneider, 2007; Sze and Kwok, 2007). The biosensing

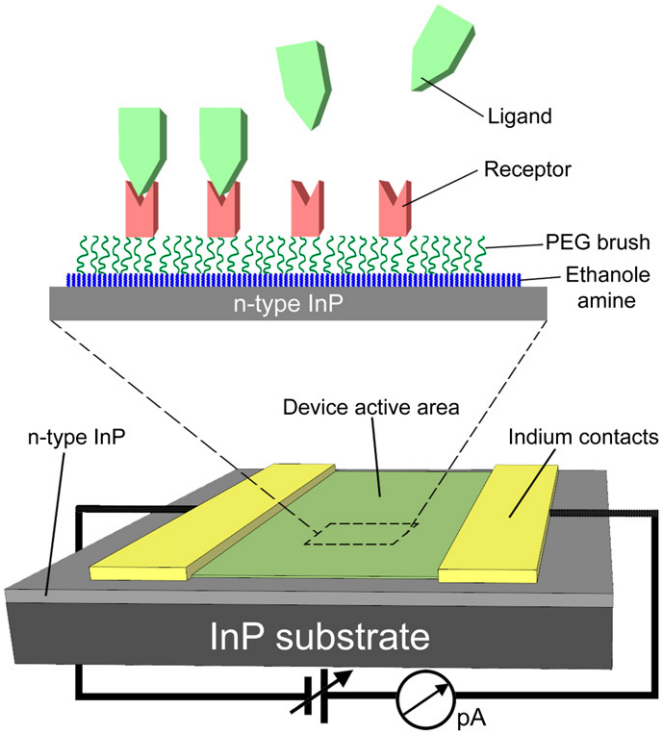

Fig. 1. Schematic presentation of the InP-biosensor setup and functionalization method via amination, PEGylation and covalent coupling of biomolecular receptor to detect specific ligand interaction via electrical resistance change measurement.

conduction channel is represented as an InP epitaxial film with indium contacts defining the active biosensing device area at which the receptor biomolecules are covalently coupled. The change in charge distribution resulting from specific receptor:ligand interactions corresponds to the gate voltage modulation on the device active area and thereby increase or decrease the overall resistance. Thus, it is possible to detect specific molecular interaction events and the amount of the ligand material by measuring the associated changes in resistance (Seker et al., 2000).

In this study we present the development and characterization of the first label-free InP biosensor for liquid environment using three different biomolecular receptor:ligand systems: i) dsDNA oligonucleotides as a highly-reproducible and comparable standard, ii) *Citrus Tristeza Virus* (CTV) capsid CB-22 protein and iii) *Xylella fastidiosa* XadA1 adhesion protein, both demonstrating a direct application to detect phytopathogens which have been associated with a large number of diseases, causing large economic losses (Chatterjee et al., 2008; Peroni et al., 2009) worldwide.

2. Material and methods

2.1. Materials

Super pure-grade materials were used, when commercially available. NHS-PEG-COOH (MW3400) was custom-synthesized by LaysanBio (USA). Semi-insulating, nominally (0 0 1) oriented InP wafers were purchased from InPAct (France). Used DNA oligonucleotides (receptor-ssDNA:5′-NH2-CCACTCGTGACGCATTCACCTCAGCAG-CACTCCTCCTCGG-3′; complementary Atto647n-fluorophor labeled ssDNA:5′-CCGAGGAGGAGTGCTGCTGAGGTGAATGCGTCACGAGTGGA-tto647n-3′; non-complementary Atto647n-fluorophor labeled ssDNA: 5′-GGCTCCTCCTCACGACGACTCCACTTACGCAGTGCTCACCAtto647n-3′) were synthesized by PURIMEX (Grebenstein, Germany). Deionized water was obtained from *Barnstead* (USA) water system (NANOpure). Goat anti-mouse and anti-rabbit antibodies conjugated with a rhodamine fluorophore were purchased from Rheabiotec (Brazil).

2.2. Indium phosphide biosensor preparation

A ~300 nm thick n-type layer of InP was grown on semi-insulating InP substrates by *Chemical Beam Epitaxy* (CBE); the layer thickness was measured by profilometry and atomic force microscopy (Cotta et al., 1995a, 1995b; Bortoleto et al., 2002). The as-grown n-type layer presents a residual electron carrier concentration of $\sim 10^{16}$ cm^{-3} (measured by Hall effect) which is commonly used for InP gas sensors (Talazac, 2001). The sample was cut into 9×8 mm^2 dimensions. The ohmic contacts using indium at the edges of the sample were annealed at 450 °C for 15 min in a nitrogen atmosphere defining the active area of the sensor device. Thin copper wires (400 μm in diameter) were welded onto the ohmic contacts and connected to the picoammeter for electrical measurements. Since the InP layers in the active region are not intentionally doped, carrier concentration can vary in the range 9.10^{15}–2.10^{16} cm^{-3} from run to run. This variation does not strongly affect the resistance of the sample which also includes the series resistance of electrical contacts. All sensor electrical measurements are normalized to rule out these effects.

2.3. Production of CB-22, Xf.XadA1 and specific antibodies

The production of the *CTV* CB-22 capsid protein, the *Xylella fastidiosa* adhesion protein Xf.XadA1 and their specific antibodies is described in the supplemental information.

2.4. Silanole generating InP pre-activation

The cleaning of the surfaces and their pre-activation is important to generate a high density of silanole groups on the surfaces, which allows surface amination through an esterification reaction. To investigate the possibility of increasing the number of silanole grafting sites by oxidation, the following treatments were performed for quantitative and qualitative comparison: i) InP directly from CBE as control, ii) Oxygen-plasma cleaning (50sccm, 200 W) for 25 min, iii) Phosphoric acid (H_3PO_4):H_2O 1:1 (v/v) for 1 min and final wash with H_2O, iv) 5 M Potassium hydroxide (KOH) for 1 min and final wash with H_2O, v) 5 min in UV (Ultraviolet) exposure and 10 min incubated in ethanol with final wash with H_2O, vi) Nitric acid (HNO_3):H_2O 1:2 (v/v) for 30 s with final wash with H_2O and vii) Methanol:HCl (Hydrogen chloride) 1:1 (v/v) for 1 min with final wash with H_2O. All surfaces were dried after treatment in a nitrogen flow.

2.5. InP surface functionalization and PEGylation

The InP biosensor supports were immersed in 5 M ethanolamine hydrochloride in water-free DMSO (Dimethyl sulfoxide) for 24 h at room temperature (RT) for homogeneous amination. The supports were then washed in dry DMSO, in ethanol and finally 5 times with water and dried in a nitrogen flow. In the second step of functionalization, the amino-reactive heterobifunctional NHS-PEG-COOH was immobilized on the supports as a linker between the surface and a biomolecule. 2 mM of the PEG linker was dissolved in water-free chloroform with 0.5% (v/v) triethylamine in which the supports were incubated for 1 h at room temperature. The supports were washed several times in water after the PEG-coating process.

2.6. Immobilization of ssDNA and antibody on PEGylated InP supports

As our standard method, amino-labeled ssDNA oligonucleotides and antibodies were immobilized to the free accessible carboxylic groups of the PEG linker via peptide binding with EDC (1-ethyl-3-(3-dimethylaminopropyl) carbodiimide) in acidic buffer as carboxyl activation substance (Walsh et al., 2001) to achieve the highest possible immobilization efficiency (Janissen et al., 2009).

Amino-labeled ssDNA oligonucleotides were immobilized on PEG-coated supports (Section 2.4) as follows: a concentration of 100 pmol/μl amino-ssDNA was used in 100 mM MES (2-(N-morpholino)ethanesulfonic acid) buffer (pH 4.75) with 50 mM EDC and with which the supports were completely covered. After 1 h reaction time at RT, the supports were washed for 5 min with pure water, 10 min in a 100 mM KCl (Potassium chloride) solution to remove physisorbed oligonucleotides and finally again 5 min with pure water and dried in a nitrogen flow. To passivate the surface against physisorption of non-complementary ssDNA the surface was blocked by incubation in blocking buffer (33% (w/v) ethylene glycol) for 15 min at 50°C. After blocking the supports were washed twice for 1 min in water.

The monoclonal 37.d.09 and polyclonal Anti-Xf.XadA1 antibodies were bound to the PEG-coated supports using 100 μg/ml in 100 mM MES buffer (pH 4.75, 50 mM EDC) covering the InP supports for 1 h at RT. Afterwards, the supports were washed twice for 10 min in PBS-TT (0.05% (v/v) Tween20, 0.2% TritonX-100 in phosphate buffer saline (PBS) buffer (pH 7.4)) to remove physisorbed antibodies. Then, the samples were washed twice for 5 min in PBS buffer (pH7.4) and the passivation of the antibody surface was carried out by covering the supports with 3% BSA (Bovine serum albumin) (w/v) in PBS buffer for 1 h at room temperature. In a final step, the supports were washed twice for 10 min with PBS-TT and twice for 10 min in PBS buffer.

2.7. Immobilization evaluation via fluorescence microscopy

The immobilization of biomolecules was investigated qualitatively and quantitatively via fluorescence detection of fluorophore-labeled specific ligands binding to the immobilized biomolecules. Specific binding was tested by immobilizing the ssDNA and antibodies in a volume defined droplet of 0.5 μl onto the PEG-coated InP surfaces (Section 2.6). To test non-specific adsorption of the specific ligands to the PEG-coated surface only, the specific ligand molecules (complementary ssDNA, CB-22 protein and Xf.XadA1 protein) were added onto the support via a drop of 20 μl which covered a wider area around the previously immobilized receptor molecules to allow simultaneous control of specific binding and unspecific adsorption.

The hybridization of complementary Atto647 n-labeled ssDNA was performed with a concentration of 10 μM on the prepared surface in 20 mM TRIS (Tris-(hydroxymethyl)aminomethane) hybridization buffer (pH 7.4) containing 100 mM NaCl (Sodium chloride) for 45 min at RT and washed afterwards in 2 × SSC (Saline-sodium citrate) buffer for 5 min, in 0.01 × SSC buffer for another 5 min to remove non-specific adsorbed ssDNA.

To analyze the antibody immobilization quality and the specific receptor:ligand binding, the immobilized CTV 37.d.09 and Anti-Xf.XadA1 antibodies were detected via antigen binding and further fluorophore labeled specific second antibodies. The CTV CB-22 and Xf.XadA1 proteins were added to the surfaces at a concentration of 10 μM in PBS buffer (pH 7.4) for 1 h at RT. Thereafter, the surfaces were washed 10 min in PBS-TT buffer and further 10 min in PBS buffer. The samples were then incubated with the specific antibodies in PBS buffer for 1 h at RT. After a washing procedure with PBS-TT and PBS of 10 min each, the fluorophore labeled second antibodies were given to the surface in BSA–PBS buffer (PBS, 3% (w/v) BSA, pH 7.4) at a concentration of 10 μM for 1 h at RT. In a final step, the samples were washed four times with PBS-TT for 10 min and twice in PBS buffer for 10 min.

The fluorescence measurements were performed using an inverted microscope (Nikon TE2000U, USA) with a peltier-cooled photon-counting EMCCD camera (Andor IXON-3, 1024 × 1024pixels, Ireland). Fluorophore excitation was achieved by a 150 W Xenon-lamp with appropriate filter sets (AHF, Germany) for the different fluorophore emission spectra of the ligand molecules. On each sample the fluorescence intensity (in photon counts/s) was measured by taking the average over five areas of 100 × 100pixels.

2.8. Conductive InP-biosensor measurements

The electrical measurements were performed in dark at RT and in appropriate buffers depending on the biomolecular system. Receptor-functionalized biosensors (Section 2.6) were deposited on a non-conductive PVC (Polyvinyl chloride) support with a liquid cell (30 μl volume) on top to guarantee that measurements were carried out on the device active area only. After system stabilization of the functionalized supports with buffer for 1 h, the conductive measurements were carried out with a voltage ramp between −100 mV and 100 mV (10 points in 2 s) calculating directly the ohmic resistance changes during the ligand titration process. The conductive measurements were performed using a *Keithley* picoamperimeter (Model 6487, USA). Before ligand titration, the resistance of the equilibrated buffer-biosensor system was measured with alternating polarization to detect any systematic errors of the system; this result will be included in the respective concentration error determination of each biomolecular system due to capacitance effects.

For each biomolecular system, specific and non-specific receptor/ligand was used to evaluate the biosensor specificity and detection resolution. For the DNA system, an Atto647n fluorophore labeled, non-complementary ligand strain was used to

analyze the non-specific adsorption quantity. For both phytopathogen antibody:antigen systems a different non-specific surface receptor was used as control. For the CTV CB-22:37.d.09 system, the Anti-Xf.XadA1 antibody was used as non-specific receptor and for the Xf.XadA1:Anti-Xd.XadA1 system the CTV 37.d.09 antibody served as non-specific receptor. The ligand was titrated for all three biomolecular systems in concentrations between 30 and 800 ng/ml. After each titration step five successive measurements were performed every 10 min until system equilibration. For analysis and biosensor response comparison, the measured resistances of each biomolecular system were normalized to the initial resistance before ligand titration ($\Delta R/R_0$).

3. Results and discussion

3.1. Covalent biomolecule immobilization and specificity

The different receptor biomolecules for specific ligand binding were successfully immobilized on functionalized InP supports in three experimental repetitions (Fig. 2). In qualitative aspect, the biomolecular surface layer is homogeneous for ssDNA (Fig. 2A), for Anti-Xf.XadA1 (Fig. 2B) and for the 37.d.09 (Fig. 2C) immobilization on oxygen plasma treated InP supports.

Quantitatively, the immobilization experiments of all three biomolecular systems show a low non-specific adsorption contingent between 6% and 8% compared to the specific binding (Fig. 2D) due to the PEG crosslinker and additional applied ethylene glycol (for ssDNA) and BSA (for antibodies) surface passivation.

In result, the developed InP functionalization and covalent biomolecule immobilization process guarantees a homogeneous, dense and functional receptor molecule layer with high passivation characteristics in reference to non-specific adsorption.

3.2. InP pre-activation effects

Amino-labeled ssDNA oligonucleotides were immobilized covalently to the PEG-coated InP supports and a complentary Atto647n-labeled ssDNA was hybridized to the surface bound ssDNA as previously described (2.7). As the functionalization efficiency depends on the amount of silanole grafting sites several common surface pre-activation methods were compared among each other by fluorescence microscopy, measuring the quantitative fluorescence intensity of five determined areas (100×100pixels) representing the amount of hybridized ssDNA. The result of two experimental repetitions is shown in Fig. 3.

In comparison, only the oxygen plasma and the HNO_3 treatment shows a significant improvement to the control. The other chemical pre-activation processes show the same amount of immobilized ssDNA as the control considering the measurement variation error. Although the maximum improvement (10%) is achieved by HNO_3 treatment, qualitative fluorescence analysis of all pre-activation methods pointed out that the control and the oxygen plasma treatment presented the most homogeneous surface coating (data not shown). As the oxygen plasma treatment causes a density improvement of about 8% to the non-treated control, the further immobilization of the different biomolecules and the electrical detection measurements were performed with oxygen-plasma treated InP supports to guarantee a high immobilization density and homogeneity leading to higher detection sensitivity and reproducibility of the biosensor.

3.3. Biosensor detection of biomolecules

The relative resistance variation measurements of the three previously described biomolecular interaction systems are shown for four experimental repetitions in Fig. 4, representing the specific receptor:ligand interaction (Fig. 4, blue points) in comparison to the unspecific receptor:ligand controls (Fig. 4, red points). Here, the

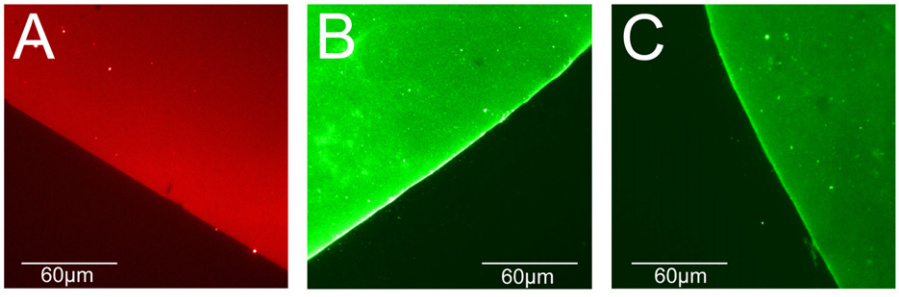

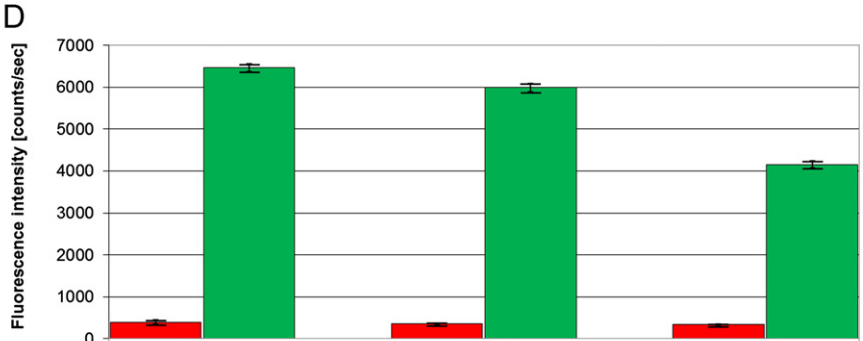

	ssDNA		XadA1		CB-22	
$\bar{x}$	397	6460	356	5987	334	4157
σ	98.8	187.4	37.4	208.8	30.8	165.8

Fig. 2. Epifluorescence measurements of immobilized (A) 40b ssDNA, (B) Xf.XadA1 antibody and (C) CTV 37.d.09 antibody on InP supports. Histogram (D) shows fluorescence intensity and standard deviation error of the specific binding areas (green) and non-specific adsorption (red), calculated for each sample ($n=3$) in 5 different areas of 100×100pixels (For interpretation of the references to color in this figure legend, the reader is referred to the web version of this article.).

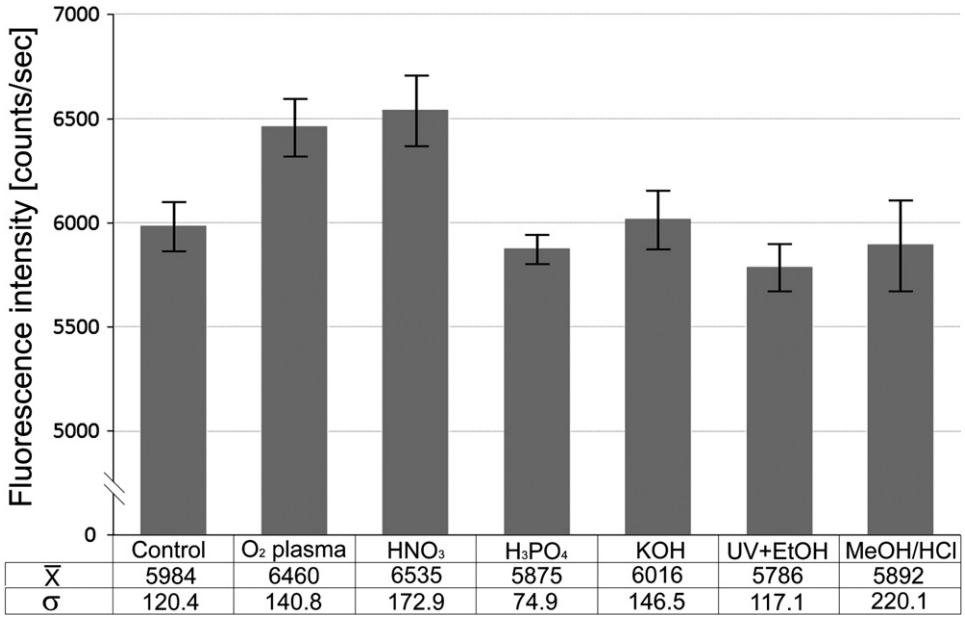

	Control	O_2 plasma	HNO_3	H_3PO_4	KOH	UV+EtOH	MeOH/HCl
$\bar{X}$	5984	6460	6535	5875	6016	5786	5892
σ	120.4	140.8	172.9	74.9	146.5	117.1	220.1

Fig. 3. Comparison of different pre-activation treatments of InP for silanole grafting-sites generation. The average fluorescence intensity (in photon counts/second) of the hybridized Atto647n-labeled ssDNA emission was measured for each sample ($n=2$) in 5 determined areas of 100 × 100pixels for each pre-activation process (No treatment [Control], Oxygen plasma [O_2 plasma], Nitric acid [HNO_3], Phosphoric acid [H_3PO_4], Potassium hydroxide [KOH], Ultraviolet irradiation with ethanol [UV+EtOH] and Methanol/Hydrochloric acid mixture [MeOH/HCl]). The mean fluorescence intensity and the standard deviation of each sample are indicated below the corresponding value bars.

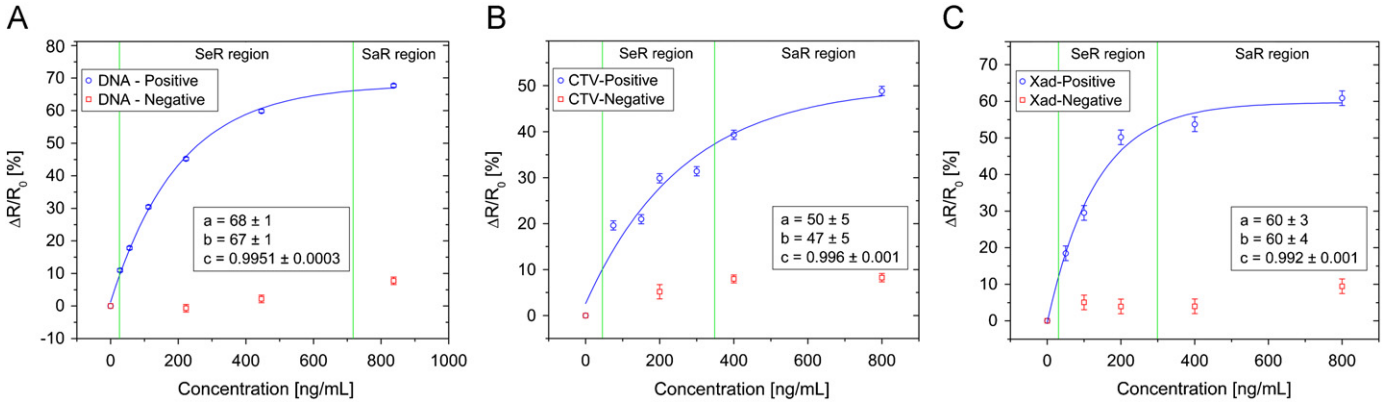

Fig. 4. Relative resistance variation ($\Delta R/R_0$) of ligand titration of the three used biomolecular receptor:ligand systems with specific receptor/ligand (blue points) and non-specific receptor/ligand (red points) as control. (A) 40 bp ssDNA:ssDNA system with non-complementary Atto647n-labeled ssDNA ligand. (B) CTV CB-22:37.d.09 antibody system with Anti-Xf.XadA1 antibody as non-specific receptor. (C) Xf.XadA1:Anti-Xf.XadA1 antibody system with CTV 37.d.09 antibody as non-specific receptor. Asymptotic saturation fitting curve ($y=a-b^*c^x$, blue line, parameters in graph) for each ligand:receptor system over n=4 samples shows saturation behavior of biosensing detection. The concentration detection limits (green lines) for the sensitive detection region (SeR) and the ligand saturation region (SaR) are shown for each biomolecular system (For interpretation of the references to color in this figure legend, the reader is referred to the web version of this article.).

combined electrical resistive changes ($\Delta R/R_0$) of all experimental repetitions showed no significant detection differences, represented by the error bars. The concentration titration for all three specific receptor:ligand systems shows a clear increase of the biosensor resistance resulting in maximum variation values about 68% for DNA:DNA, 60% for Xf.XadA1:Anti-Xf.XadA1 and 50% for CB-22:37.d.09, whereas the unspecific receptor:ligand measurements shows non-specific adsorbed DNA/antigens and non-correlated resistance variations with the concentration up to approximately 10% for all three biomolecular systems.

The specific interaction measurements follow a saturation behavior for all three systems, which can be fitted asymptotically (Fig. 4, blue curves) to gain detailed information about sensitivity and error propagation (the procedure is described in detail in the supplemental information). Briefly, using the fitting parameters (Fig. 4, insets), the sensitivity defining error for each measured biomolecular system was calculated by asymptotic saturation fitting ($y=a-b^*c^x$, Draper and Smith, 1988). The error value represents the minimal detection concentration (Table 1, MCE) resulting in 4 ng/ml for ssDNA, 18 ng/ml for Xf.XadA1 and 32 ng/ml for CB-22 detection.

Table 1
Calculated minimal detection concentration (MCE) and defined sensitivity regions for each biomolecular system (NsR: Non-specific region, SeR: Sensitive region, SaR: Saturation region) including the mean concentration error (σ) in [ng/ml].

	MCE (ng/ml)	NsR (ng/ml)	SeR (ng/ml)	SaR (ng/ml)
40 bp DNA	4 ($\sigma=2$)	< 30 (1 pM)	30∼715	> 715
Xylella fastidiosa	18 ($\sigma=9$)	< 34 (1.9 nM)	34∼250	> 250
Citrus Tristeza Virus	32 ($\sigma=16$)	< 60 (2.3 nM)	60∼340	> 340

These concentration errors were used to estimate three sensibility regions (Table 1). i) The non-specific region (NsR) which is determined by the maximum concentration of adsorbed non-specific ligand in which the biosensor response cannot differentiate between a specific and non-specific receptor:ligand interaction; ii) the sensitive region (SeR) where it is possible to measure clearly the concentration of the specific ligand and iii) the saturation region (SaR) which shows specific receptor:ligand interactions only as an *on-off* behavior.

In particular, the ssDNA receptor:ligand system was chosen as a positive control sample for the biosensor evaluation, as it represents a simple and strong reproducible biomolecular interaction system. Due to the small size of the ssDNA oligonucleotides resulting in a shorter diffusion time compared to the protein systems and uniform charge distribution, this system shows a very small detection concentration (Table 1, MCE) and provides a wide sensitivity region between 30ng/ml and 715 ng/ml for reliable quantitative concentration determination (Table 1, SeR). In contrast, the minimal detection concentration (Table 1, MCE) of both protein:antibody systems shows a larger variance and consequently a smaller sensitive region range due to the larger molecule size and their non-uniform surface charge distribution, which are 60 ng/ml–340ng/ml for the CB-22 and 34 ng/ml–250 ng/ml for the Xf.XadA1 system.

The quantitative comparison with biosensors described in literature is difficult due to several factors as different transduction modes, molecule size and surface charge variations, charge distribution changes upon binding, molecular surface density and the functionalization method of the device active area itself (Nicu and Leïchlé, 2008). By presenting here the first InP based biosensor the comparison is restricted to considering the minimum detection concentration and resolution limit.

The Enzyme Linked Immunosorbent Assay (ELISA) represents the standard method for specific molecular receptor:ligand interactions in medical and biological research as well as common phytopathogen infection diagnostics using luminescence emission of additional bound antibodies. This optical detection based approach needs a minimum ligand concentration of 2 mg/ml for reliable detection for the same CTV system (Peroni et al., 2009) used in this study. Hence, two orders of magnitude higher than that necessary for our assay; moreover, our biosensor detection method needs no additional specific labeling. The Polymerase Chain Reaction (PCR) method is an additional tool for pathogen diagnosis nowadays (Khoodoo et al., 2005). Reliable detection was achieved by a minimum DNA material concentration of 1.2 μg/ml (2.41 μM). In comparison to the presented DNA detection performance, we achieved binding proof with a concentration two orders of magnitude lower (1 pM).

An analog FET-like operating detection platform based on amorphous silicon (a-Si:H) for label-free detection of dsDNA in literature (Gonçalves et al., 2008) shows a minimal detection concentration of 50 nM. This represents an amount for reliable detection four orders of magnitude higher than for our InP biosensor (1 pM). Moreover, reported highly-sensitive microbial detection focused on electrochemical antibody:antigen detection approaches require a minimum concentration of ~1 nM (Lei et al., 2005) which is comparable to our developed InP based sensing technique with a limit of 1.9 nM.

4. Conclusions

In this work an optimized functionalization and biomaterial immobilization procedure allowed us to develop the first highly-sensitive and label-free InP based resistive biosensor. Important characterization, such as biomolecular conjugation efficiency, detection concentration limits, receptor:ligand specificity and concentration detection range was analyzed by using three different biological systems: i) synthetic dsDNA, ii) *Citrus Tristeza Virus* capsid protein and iii) *Xylella fastidiosa* host surface adhesion protein.

The high detection sensitivity of about 2 nM for phytopathogenic diagnosis can be compared with the most sensitive biosensing methods using an electrochemical approach. Beside the desirable sensitivity, the advantage of the developed biosensor is the effortless application and direct molecular detection without the need of additional labeling. Since the severe CB-form (*Capão bonito*) of *Citrus Tristeza Virus* and *Xylella fastidiosa* used in this study represent agriculture plagues, this device could be useful for early infection detection, avoiding the disease spreading in the orchards.

Taken altogether, the results from this study provide a great approach to highly-sensitive InP based sensors for diagnostics in environmental and life sciences. In further development stages, the specificity could be enhanced by using arrays of miniaturized InP biosensors with several receptors for a specific pathogen or receptors for various pathogens to develop a mobile platform for rapid and easy field diagnosis.

Acknowledgments

This work was financially supported by FAPESP (Fundação de Amparo a Pesquisa do Estado de Sao Paulo) and CNPq (Conselho Nacional de Desenvolvimento Científico e Tecnológico). A.L.D.M. and R.J. acknowledge scholarships from CNPq and FAPESP, respectively.

Appendix A. Supplementary information

Supplementary information associated with the production of the proteins and antibodies which were used within this study can be found in the online version at http://dx.doi.org/10.1016/j.bios.2012.03.038.

References

Albrecht, C., Blank, K., Lalic-Mülthaler, M., Hirler, S., Mai, T., Gilbert, I., Schiffmann, S., Bayer, T., Clausen-Schaumann, H., Gaub, H.E., 2003. Science 301, 367–370.
Blank, K., Mai, T., Gilbert, L., Schiffmann, S., Rankl, J., Zivin, R., Tackney, C., Nicolaus, T., Spinnler, K., Oesterhelt, F., Benoit, M., Clausen-Schaumann, H., Gaub, H.E., 2003. Proceedings of the National Academy of Science 100, 11356–11360.
Bortoleto, J.R.R., Cotta, M.A., de Carvalho, M.M.G., 2002. Surface Science 515, 117–125.
Chatterjee, S., Almeida, R.P.P., Lindow, S., 2008. Annual Review of Phytopathology 46, 243–271.
Chattopadhyay, S., Ganguly, A., Chen, K.H., Chen, L.C., 2009. Critical Reviews in Solid State and Materials Sciences 34, 224–279.
Cotta, M.A., Hamm, R.A., Chu, S.N.G., Harriott, L.R., Temkin, H., 1995a. Applied Physics Letters 66, 2358–2360.
Cotta, M.A., de Carvalho, M.M.G., Pudenzi, M.A.A., Landers, K.M.I., de Souza, C.F., Landers, R., Teschke, O., 1995b. Applied Physics Letters 67, 1122–1124.
Draper, N.R., Smith, H., 1988. Applied Regression Analysis, third ed. Wiley Interscience, New York.
Ebner, A., Hinterdorfer, P., Gruber, H.J., 2007. Ultramicroscopy 107, 922–927.
Galup-Montoro, C., Schneider, M.C., 2007. MOSFET modeling for circuit analysis and design. World Scientific, London/Singapore.
Gonçalves, D., Prazeres, D.M., Chu, V., Conde, J.P., 2008. Biosensors and Bioelectronics 24, 545–551.
Hinterdorfer, P., Gruber, H.J., Kienberger, F., Kada, G., Riener, C., Borken, C., Schindler, H., 2002. Colloids and Surfaces B: Biointerfaces 23, 115–123.
Jane, A., Dronov, R., Hodges, A., Voelcker, N.H., 2009. Trends Biotechnology 27, 230–239.
Janissen, R., Oberbarnscheidt, L., Oesterhelt, F., 2009. Colloids and Surfaces B: Biointerfaces 71, 200–207.

Kamruzzahan, A.S., Ebner, A., Wildling, L., Kienberger, F., Riener, C.K., Hahn, C.D., Pollheimer, P.D., Winklehner, P., Hölzl, M., Lackner, B., Schörkl, D.M., Hinterdorfer, P., Gruber, H.J., 2006. Bioconjugate Chemistry 17, 1473–1481.
Khoodoo, M.H.R., Sahin, F., Jaufeerally-Fakim, Y., 2005. European Journal of Plant Pathology 112, 379–390.
Kimura, T., Hasegawa, H., Sato, T., Hashizume, T., 2006. Japanese Journal of Applied Physics 45, 3414–3422.
Krautbauer, R., Rief, M., Gaub, H.E., 2003. Nano Letters 3, 493–496.
Lazcka, O., Del Campo, F.J., Muñoz, F.X., 2007. Biosensors and Bioelectronics 22, 1205–1217.
Lei, Y., Mulchandani, P., Wang, J., Chen, W., Mulchandani, A., 2005. Environmental Science and Technology 39, 8853–8857.
Lenci, S., Tedeschi, L., Domenici, C., Lande, C., Nannini, A., Pennelli, G., Pieri, F., Severi, S., 2010. Materials Science and Engineering: C 30, 1221–1226.
Lindroos, K., Liljedahl, U., Raitio, M., Syvänen, A.C., 2001. Nucleic Acids Research 29, e69–9.
Logatcheva, A., Horton, J.H., 2008. Colloids and Surfaces: A 315, 156–164.
Nicu, L., Leïchlé, T., 2008. Journal of Applied Physics 104, 111101–111117.
Park, H.H., Ivanisevic, A., 2007. The Journal of Physical Chemistry C 111, 3710–3718.
Peroni, L.A., Lorencini, M., dos Reis, J.R., Machado, M.A., Stach-Machado, D.R., 2009. Virus Research 145, 18–25.
Sato, T., Mizohata, A., Hashizume, T., 2010. Journal of The Electrochemical Society 157 (2), 165–169.
Seker, F., Meeker, K., Kuech, T.F., Ellis, A.B., 2000. Chemical Reviews 100, 2505–2536.
Sturzenegger, M., Prokopuk, N., Kenyon, C.N., Royea, W.J., Lewis, N.S., 1999. Journal of Physical Chemistry: B 103, 10838–10849.
Su, L., Jia, W., Hou, C., Lei, Y., 2011. Biosensors and Bioelectronics 26, 1788–1799.
Sze, S.M., Kwok, K., 2007. Physics of Semiconductor Devices, third ed. Wiley, New Jersey.
Talazac, L., 2001. Sensor and Actuators: B 76, 258–264.
Vandenberg, E.T., Bertilsson, L., Liedberg, B., Uvdal, K., Erlandsson, R., Elwing, H., Lundström, I., 1991. Journal of Colloid and Interface Science 147, 103–118.
Walsh, M.K., Wang, X., Weimer, B.C., 2001. Journal of Biochemical and Biophysical Methods 47, 221–231.
Wang, D., Jones, F.R., Denison, P., 1992. Journal of Materials Science 27, 36–48.
Wang, D., Jones, F.R., 1993. Journal of Materials Science 28, 2481–2488.
Wierzbowska, K., Bideux, L., Adamowicz, B., Pauly, A., 2008. Sensors and Actuators: A 142, 237–241.
Xue, Q., Bian, C., Tong, J., Sun, J., Zhang, H., Xia, S., 2011. Sensors and Actuators A 169, 282–287.
Yong-Mei, X., Zhi-Shan, H., Onnop, S., Ayse, B., Erdogan, G., 2007. Journal of Chemical Technology & Biotechnology 82, 33–38.
Zerulla, D., Chassé, T., 2009. Journal of Electron Spectroscopy and Related Phenomena 172, 78–87.

Highly-sensitive and label-free Indium Phosphide biosensor for early phytopathogen diagnosis

Supplemental information

1. Cloning, expression and purification of Xf.XadA1 membrane protein

The *xfxadA1* sequence ORF Xf1257 (3015bp) which encodes the *Xylella fastidiosa* surface adhesion protein Xf.XadA1 (1005 aa) was amplified by PCR (polymerase chain reaction) from *X. fastidiosa* genomic DNA using specific primers. The "head" domain of Xf.XadA1, beginning at position 50aa and ending at position 225aa, was constructed using the primers $XadA1_{forward}$ (5'-CATAGCTAGCGGTCTTGCGCTTACAA-3') and $XadA1_{reverse}$ (5'-TGGAATTCGGCAATCG TCTTCACC-3') containing the *Nhe*I and *Eco*RI restriction enzyme sites, respectively. The PCR amplification product was cloned into the expression vector pET28a(+) (Novagen, USA) in which was included an additional N-terminal six-histidines tag and a thrombin protease site to the coding sequence using the *Nhe*I and *Eco*RI restriction sites. The cloned domains were overexpressed in *E. coli* C43 (DE3) (Avidis) strain. Cells were grown at 37ºC in 1 liter of LB (Lysogeny broth) medium, supplemented with 0.2% glucose and containing kanamycin (30 µg/mL) until optical absorbance of DO_{600} of 0.6–0.8 was reached. Recombinant proteins were induced by the addition of 1 mM IPTG (isopropyl-β-d-1-thiogalactopyranoside) followed by cultivation for 4 h at 25ºC and 200 rpm. The culture were harvested by centrifugation (3000 *g*, 15 min, 4 ºC), and sedimented cells were resuspended in 50 mL of buffer A (50 mm Tris-HCl, 150 mm NaCl, pH 8.0) plus 1 mg/mL lysozyme and 1 mM phenylmethanelsulfonylfluoride (Sigma, St Louis, USA) and incubated for 30 min on ice. The lysates were disrupted by sonication and the unbroken cells and debris were removed by centrifugation (27000 *g*, 40 min, 4ºC). The Xf.XadA1 protein purification was performed by affinity chromatography using a Nickel-NTA (Nitrilotriacetic acid) column (Qiagen, Hilden, Germany), equilibrated with buffer A. The purified proteins were eluted with five column volumes of buffer A containing 250 mM imidazole and the degree of purity was estimated by SDS-PAGE (sodium dodecyl sulfate polyacrylamide gel electrophoresis). Subsequently, the purification step the N-terminus His_6-tag of recombinant proteins were removed using a thrombin cleavage kit (Novagen, USA).

2. Cloning, expression and purification of CTV CB-22 protein

The production of the CTV CB-22 is described in detail in literature (Peroni *et al.*, 2009). Shortly, CTV dsRNA was isolated from a 19-year-old Pêra sweet orange tree grafted on Rangpur lime. The cDNA synthesis and amplification of the coat protein (CP) gene were performed and the CP gene was amplified by PCR using specific primers: CN119 5´-AGATCTACCATGGACGACGAAACAAAG-3´ and CN120 5´-GAATTCGCGGCCGCT CAACGTGTGTTAAATTTCC-3´, containing *EcoRI* and *BglII* restriction sites at the 5´ end of the forward and reverse primers, and were cloned into the pBluescript KS+ vector. The CB-22 clone was sequenced and expressed in pET22. The DNA of the CB-22 clone was isolated by phenol extraction and sequenced with BigDye chemistry on an ABI Prism 3700 Automated sequencer (Applied Biosystems, USA). The expression of recombinant protein was induced at an early logarithmic phase by the addition of 100mM IPTG (Isopropyl-d-thiogalactopyranoside) under constant agitation during 5 h at 37°C. Aliquots (5 mL) of this culture were centrifuged at 6000×*g* for 15min, the pellet was suspended in 300µL SDS-PAGE sample buffer (0.062M Tris/HCl, pH 6.8; 10% Glycerol; 2% SDS; 5% β-Mercaptoethanol and 0.02% Bromphenol blue) and frozen at -20°C until usage.

For purification, the expressed CP proteins were subjected to electrophoresis in 12.0% polyacrylamide gels under denaturing conditions. The proteins were precipitated with 0.25M KCl and 1mM DTT (Dithiothreitol) and the recombinant proteins were identified by comparing with a negative standard (*E. coli DH5* without IPTG induction). Gel slices containing proteins were transferred to dialysis tube containing 1.0mL of 0.2M Tris/acetate, pH 7.4, 10% SDS, 100mM dithiothreitol per 0.1 g of wet polyacrylamide gel. The dialysis tube was crosswise in a horizontal electrophoresis chamber (Pharmacia LKA-GNA 200) containing the running buffer (50mM Tris/acetate pH 7.4; 0.1% SDS; 0.5mM sodium thioglycolate) and run at 30V for 60 min. The proteins were concentrated by ultracentrifugation at 4000×*g* during 25 min, using Centriprep-10 system (Amicon®, Millipore, Billerica, MA, USA).

3. Antibody production

The *Citrus Tristeza Virus* monoclonal antibody 37.d.09 was produced by using female BALB/c mice (an albino, laboratory-bred strain of the House Mouse) based on the protocol of Peroni *et al.* (2009). In summary, the recombinant CB-22 protein was mixed (v/v) with Freund's complete adjuvant (FCA) or Freund's incomplete adjuvant (FIA) (Sigma) and injected into individual mice on day 0 (20 µg, FCA), 14 (20 µg, FIA), 21 (10 µg), FIA) and one booster dose on day 32 (10 µg, PBS, pH 7.3). The response to the immunized antigen was assessed by measuring the antibody titer in mouse serum by indirect ELISA. Mice with the highest titer were splenectomized at day 4 after the booster injection. The spleen cells were fused with SP2/0- Ag14 myeloma cells. Culture fluids from the hybridoma cells were screened using Double Antibody Sandwich Indirect ELISA (DASI-ELISA) assays and only positive clones producing specific antibodies were selected. Finally, the monoclonal antibodies IgGs were purified by protein affinity chromatography (Pierce, Thermo Forma, USA).

The *Xylella fastidiosa* polyclonal antibody (Anti-Xf.XadA1) was obtained by immunization of New Zealand White rabbits from Caserta *et al.* (2010). Briefly, the purified protein was mixed with Freund's complete adjuvant (Sigma) and injected into individual rabbits. Proteins mixed with Freund's incomplete adjuvant were injected two more times, at 10 and 20 days after the first injection. The concentration of inoculated proteins was 150 µg. The quality of the antibodies was tested by performing a direct enzyme-linked immunosorbent assay (ELISA), using the target proteins as antigens and PBS as the negative control.

4. Minimal detection concentration (MCE) calculation

For each measured biomolecular system the minimal detection concentration of the specific ligand (MCE, Table 1) was calculated by taking into account all 10 acquisitioned data points [$\Delta R/R_0$] for each repetition (40 data points in total) of each individual ligand titration step. As the titration results show a ligand saturation behavior for each tested biomolecular system, an asymptotic saturation fitting ($y=a-b*c^x$) was applied (Figure 4, blue curves). This equation was used to calculate an average sensor response error, defined by the fitting parameters a, b and c and their respective standard deviations (Figure 4, insets; Draper and Smith, 1988), as well as by the concentration in the solution. For simplicity, we considered a constant sensor response error for the average concentration in the range used in our experiment. The fitting equation was again used to find the mean concentration errors, (σ = ±2, ±9 and ±16 ng/ml for DNA, Xad and CTV, respectively) shown in Table 1. Finally, the minimal detection concentration (MCE) is thus defined according to this error bar. In order to clearly distinguish between two measurement points, there should be a minimum overlap between their error bars; this condition is fulfilled if we consider twice the concentration error ($2*\sigma$) which leads to the MCE value for each specific receptor:ligand system. The same reasoning is applied to the NsR (non-specific region), SeR (sensitive region) and SaR (saturation region) regions of the sensor detection behavior shown in Table 1.

References:

Caserta, R., Takita, M.A., Targon, M.L., Rosselli-Murai, L.K., de Souza, A.P., Peroni, L., Stach-Machado, D.R., Andrade, A., Labate, C.A., Kitajima, E.W., Machado, M.A., de Souza, A.A., 2010. Applied and Environmental Microbiology 74(17), 4250–4259.

Peroni, L.A., Lorencini, M., Ribeiro dos Reis, J.R., Machado, M.A., Stach-Machado, D.R., 2009. Virus Research 145, 18-25.

Draper, N. R., Smith, H., 1988. Applied Regression Analysis, third ed., John Wiley & Sons, New Jersey.